Proc. Natl. Acad. Sci. USA
Vol. 93, pp. 7612–7617, July 1996
Biophysics

Increased tricarboxylic acid cycle flux in rat brain during forepaw stimulation detected with ^{1}H [^{13}C] NMR

FAHMEED HYDER*†, JENNIFER R. CHASE*, KEVIN L. BEHAR‡, GRAEME F. MASON§, MOHAMED SIDDEEK*, DOUGLAS L. ROTHMAN¶, AND ROBERT G. SHULMAN*

Departments of *Molecular Biophysics and Biochemistry, ‡Neurology, and ¶Internal Medicine, Yale University, New Haven, CT 06520-8043; and §Center for Nuclear Imaging, University of Alabama, Birmingham, AL 35294-4470

Contributed by Robert G. Shulman, March 1, 1996

ABSTRACT **NMR spectroscopy was used to test recent proposals that the additional energy required for brain activation is provided through nonoxidative glycolysis. Using localized NMR spectroscopic methods, the rate of C4-glutamate isotopic turnover from infused [1-^{13}C]glucose was measured in the somatosensory cortex of rat brain both at rest and during forepaw stimulation. Analysis of the glutamate turnover data using a mathematical model of cerebral glucose metabolism showed that the tricarboxylic acid cycle flux (V_{TCA}) increased from 0.49 ± 0.03 at rest to 1.48 ± 0.82 μmol/g/min during stimulation ($P < 0.01$). The minimum fraction of C4-glutamate derived from C1-glucose was ≈75%, and this fraction was found in both the resting and stimulated rats. Hence, the percentage increase in oxidative cerebral metabolic rate of glucose use (CMR_{glc}) equals the percentage increases in V_{TCA} and cerebral metabolic rate of oxygen consumption (CMR_{O2}). Comparison with previous work for the same rat model, which measured total CMR_{glc} [Ueki, M., Linn, F. & Hossman, K. A. (1988) *J. Cereb. Blood Flow Metab.* 8, 486–494], indicates that oxidative CMR_{glc} supplies the majority of energy during sustained brain activation.**

It has been generally believed that, under normal physiological conditions in the adult mammalian brain, almost all the energy required for ATP generation is supplied by oxidation of glucose through the tricarboxylic acid (TCA) cycle (1). However, more recent human studies using positron emission tomography during visual stimulation (2, 3) reported a greater localized increase of the cerebral metabolic rate of glucose use (CMR_{glc}) compared with that of oxygen consumption (CMR_{O2}). This loss of stoichiometry between CMR_{glc} and CMR_{O2} has been qualitatively consistent with the finding of elevated lactate during somatosensory stimulation of the rat cortex (4) and visual stimulation of the human cortex (5, 6). However, the increase in lactate is small and/or transient in contrast to the large change predicted from the positron emission tomography findings (7). To date, it remains unclear whether nonoxidative glycolysis is a major energy source for sustained cortical activation (7).

In a study by [^{14}C]deoxyglucose autoradiography, Ueki and coworkers (4) reported that, during electrical stimulation of the rat forepaw, both CMR_{glc} and cerebral blood flow (CBF) increased in the contralateral somatosensory area. The additional finding that the concentration of lactate increased led them to conclude that glucose oxidation was incomplete during brain activation (4). However, CMR_{O2} was not measured in this study (4), so the mismatch between CMR_{glc} and CMR_{O2} was not determined quantitatively.

NMR spectroscopy can be used to determine the TCA cycle flux (V_{TCA}) in the brain by measuring the rate of ^{13}C-label flow from C1-glucose to C4-glutamate (8–10). Here, we present the rate of glutamate ^{13}C isotopic turnover data localized by functional MRI (fMRI) to the region activated during forepaw stimulation (11). We have shown by fMRI that activation during this stimulation is confined to the contralateral motor and somatosensory areas (11), in agreement with the autoradiography study (4). A mathematical model of cerebral glucose metabolism (12, 13) was fitted to the present glutamate ^{13}C isotopic data to calculate V_{TCA} at rest and during forepaw stimulation. The complete measurements in this study allowed us to calculate the oxidative portion of CMR_{glc} as well as CMR_{O2} from V_{TCA}, both at rest and during stimulation. We show that, within experimental accuracy, the percentage increases in oxidative CMR_{glc} and CMR_{O2} are similar to the percentage increase in total CMR_{glc} measured by autoradiography (4). We conclude that, during sustained rat forepaw stimulation, oxidative glycolysis is the major energy source for cortical activation. Preliminary accounts of this work have been presented elsewhere (14).

MATERIALS AND METHODS

Animal Preparation. Adult, male, Sprague–Dawley rats (175–375 g, fasted 24 h) were tracheotomized and ventilated with a mixture of 70:30 N_2O/O_2 under α-chloralose anesthesia administered i.p. (20 mg/kg/0.5 h). A femoral artery was cannulated for periodic sampling and measurement of blood gases, pH, pressure, and glucose. Physiological variables were maintained within normal limits by small adjustments in ventilation [P_aCO_2 = 29–38 mmHg (1 mmHg = 133 Pa); P_aO_2 = 130–145 mmHg; pH = 7.36–7.41; blood pressure = 75–95 mmHg]. For other details of animal preparation, see refs. 4, 9, and 11. A pair of copper electrodes (≈6 mm long, ≈1 mm in diameter) were inserted into the skin of both forepaws (between digits 1 and 2 and digits 3 and 4). An electrical stimulator (Harvard Apparatus) provided 5-V square-wave pulses of 0.3-ms duration at 3 Hz (4, 11). Brain glutamate ^{13}C labeling was achieved by an i.v. infusion of D-[1-^{13}C]glucose (99 atom %; Mercke Sharp & Dohme) at a rate that resulted in an elevated and stable plasma glucose level (9). The infusion began 6–10 min after the start of the stimulation to permit cerebral metabolism to attain a new steady state. Plasma samples (50–100 μl) were drawn every 15 min for quantitation (15, 16) of the concentration and ^{13}C fractional enrichment (FE) of C1-glucose.

NMR Spectroscopy. *In vivo* NMR data were acquired using a 7 Tesla horizontal-bore spectrometer (Bruker, Billerica,

The publication costs of this article were defrayed in part by page charge payment. This article must therefore be hereby marked "*advertisement*" in accordance with 18 U.S.C. §1734 solely to indicate this fact.

Abbreviations: TCA, tricarboxylic acid; CMR_{glc}, cerebral metabolic rate of glucose use; CMR_{O2}, cerebral metabolic rate of oxygen consumption; V_{TCA}, tricarboxylic acid cycle flux; CBF, cerebral blood flow; fMRI, functional MRI; FE, fractional enrichment; POCE, proton-observed carbon-13-edited; BOLD, blood-oxygenation level dependent.

†To whom reprint requests should be addressed at: Magnetic Resonance Center, Yale University, P.O. Box 208043, New Haven, CT 06520-8043. e-mail: hyder@mrcbs.med.yale.edu.

MA) equipped with actively shielded shim/gradient coils and operating at 300.8 MHz for ^{1}H and 75.2 MHz for ^{13}C. The surface-coil radio-frequency probe consisted of a ^{1}H transceiver coil (8 mm in diameter) and a concentric ^{13}C coil (20 mm in diameter) for ^{13}C inversion and decoupling. To identify the anatomical regions activated by forepaw stimulation, multislice functional images were acquired during forepaw stimulation with a T_2^*-weighted echo-planar imaging sequence (17) in separate experiments (n = 4). Other details of fMRI are discussed elsewhere (11). Coordinates for the placement of a 50-mm^3 rectangular volume of interest for the proton-observed, carbon-13-edited (POCE) NMR experiments were based on the regions activated in the fMRI experiments. Experimental details of the localized POCE NMR method have been described (8–10, 18). The magnetic field homogeneity of the volume of interest was optimized (19). Localized POCE NMR pulse sequence included inversion-recovery water suppression, volume of interest selection (ref. 20; $x \times y \times z = 7 \times 1.5 \times 5$ mm), and POCE (8–10). The POCE segment of the sequence consisted of a spin-echo: a ^{1}H-90° composite pulse ($\theta_y\theta_x\theta_{-y}\theta_x$) followed by a ^{1}H-180° 2-τ-2 semiselective pulse ($\theta_x\theta_x$; τ = 676 μs). The spin-echo delay time was 20 ms. Two balanced crusher gradients were used in each half of the spin-echo sequence to eliminate non-refocusing magnetization (10, 18). A ^{13}C-180° phase-cycled pulse ($\theta_x\theta_{\pm x}$; 375 μs) was centered at 1/2J [4 ms; $J \approx$ 125 Hz (8–10)] from the ^{1}H-90° pulse. Each free-induction decay was acquired in the presence of a broadband (±20 ppm) ^{13}C decoupling composite pulse ($\theta_x 2\theta_y\theta_x$; 550 μs) within the acquisition time (204.8 ms). The frequencies of the ^{13}C inversion and decoupling pulses were optimized for the C4-glutamate resonance (2.35 ppm). The recycle time for each scan was 2 s. These acquisition parameters corresponded to a duty cycle of 7% with ≈2 W of power deposited for the ^{13}C inversion and decoupling pulses. The ^{13}C inversion pulse, which was applied in alternate scans by alteration of its phase ($\theta_x\theta_{\pm x}$), resulted in 95% inversion with a bandwidth of ±2.5 ppm (in ^{1}H chemical shift) based on *in vitro* samples of [2-^{13}C]acetate and glycine. Consecutive free-induction decays, with and without ^{13}C inversion, were collected in two different memory blocks (40 scans per block). Before Fourier transformation, one block was subtracted from the other, zero-filled, and exponentially line-broadened (15–20 Hz). The POCE NMR difference-spectrum was phase corrected between 4.0–0.5 ppm (zero- and first-order phase corrections). NMR experiments were carried out under resting and stimulated conditions and in three different regions of the cortex [motor (n = 4), somatosensory (n = 11), and occipital (n = 6)].

Brain Extracts. After the completion of each *in vivo* POCE experiment, the rat brain was frozen in liquid nitrogen and removed from the skull. Regions and volumes of the cortex identical to those in the *in vivo* NMR study (see above) were sliced (30–50 mg) based on a rat brain atlas (21), and amino acids were extracted (15, 16). POCE NMR spectra were obtained (8.4 Tesla, Bruker) to determine the ^{13}C FE of C4-glutamate (see refs. 15 and 16 for details). Each *in vivo* POCE time course was then converted to a time course of ^{13}C FE of C4-glutamate.

Metabolic Modelling. V_{TCA} was calculated using a metabolic model (refs. 12 and 13; Fig. 1), with inputs consisting of the time courses of measured plasma glucose concentration, and ^{13}C FEs of C1-glucose and C4-glutamate. The model describes the ^{13}C-label flow from C1-glucose to C3-pyruvate (and C3-lactate), via the TCA cycle intermediates, and into C4-glutamate due to a fast isotopic exchange between C4-glutamate and C4-α-ketoglutarate. V_{TCA} is calculated from the rate of ^{13}C isotopic turnover of the glutamate pool (see refs. 12 and 13). The model iterates the value of V_{TCA} to find the best fit to the data. The precision of each measurement was assessed by adding random noise to the best fit (12, 13). The model assumptions were similar to those in ref. 12 and where

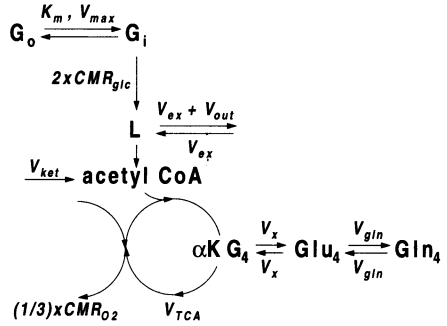

FIG. 1. Schematic representation of the metabolic model (12, 13). The [1-^{13}C]glucose in the plasma (G_o) and the brain (G_i) exchange via Michaelis–Menten kinetic parameters K_m (13.9 mM) and V_{max} (1.16 μmol/g/min). The ^{13}C label flows at the rate 2 × CMR_{glc} through the glycolytic intermediates (negligible concentrations) and arrives at C3-pyruvate (+ C3-lactate), represented by L (1.5 μmol/g). There is an exchange of blood–brain pyruvate (and lactate), V_{ex}, which is a source of unlabeled carbon into the TCA cycle. Another source of unlabeled carbon that enters the TCA cycle is the ketone body flux, V_{ket}, which also dilutes the ^{13}C FE of intermediates in the TCA cycle. The flux of total dilution of the acetyl-CoA pool, V_{dil}, which is the sum of V_{ket} and V_{ex}, was set to 0.25 × V_{TCA}. The efflux at L, V_{out}, causes some ^{13}C label to be lost to the blood and was assumed to be negligible. The ^{13}C label enters the TCA cycle and labels C4-α-ketoglutarate, αKG_4, and C4-glutamate (12.0 μmol/g), Glu_4. These two pools are in very rapid isotopic exchange, V_x (where $V_x/V_{TCA} \gg 1$; see refs. 12 and 13). Also, there is an exchange between C4-glutamate and C4-glutamine (6.2 μmol/g), Gln_4, at a rate of V_{gln} (0.08 μmol/g/min). One turn of the TCA cycle, V_{TCA}, is approximately coupled with $\frac{1}{3}$·CMR_{O2}. A set of coupled differential equations are used to describe the model, and an iterative method is used to fit the model to the C4-glutamate data. See refs. 12 and 13 for further details.

it was shown that the sensitivity of the calculated value of V_{TCA} to assumptions in the model is negligible (12, 13).

Two parameters have secondary effects on the calculated value of V_{TCA}. First, the brain glucose concentration contributes to the time lag before the label reaches the glutamate pool. Brain glucose levels used for the modelling were calculated using measured plasma glucose concentrations and previously determined Michaelis–Menten glucose transport parameters in rat brain (K_m = 13.9 mM; V_{max}/CMR_{glc} = 5.8, where K_m is the half-saturation concentration for transport and V_{max} is the maximum transport rate; ref. 16). The modelling was performed with V_{max} set to 1.16 or 4.64 μmol/g/min based on a range of values of V_{max}/CMR_{glc} (5.8 and 23.2, respectively; ref. 16). Second, the rate of ^{13}C-label exchange between C4-glutamate and C4-glutamine, V_{gln}, can affect the calculated value of V_{TCA}. The modelling was performed with V_{gln} set to 0.08 or 0.44 μmol/g/min based on a range of values calculated from an *in vivo* ^{13}C NMR study (22) of the resting rat brain under similar conditions. Pool sizes of glutamate, glutamine, and pyruvate+lactate were assumed to be 12.0, 6.2, and 1.5 μmol/g, respectively, as measured previously (16, 23). Based on phantom studies, the C4-glutamate peak was assumed to have contribution from 25% of the C4-glutamine peak.

If glucose is the only source of carbon for the TCA cycle and all the [1-^{13}C]glucose enters the acetyl-CoA pool, then the stoichiometry of fluxes for the breakdown of glucose is given by

$$CMR_{glc} = \tfrac{1}{2} \times V_{TCA}, \quad [1]$$

$$CMR_{O2} = 3 \times V_{TCA}, \quad [2]$$

as shown in Fig. 1. The ^{13}C FE of C4-glutamate should be exactly half that of C1-glucose (12, 13). However, experimentally we find that ^{13}C FE of C4-glutamate is less than half that of C1-glucose (9, 24). Two metabolic pathways that may contribute to the dilution of C4-glutamate are ^{12}C influxes

from ketone bodies, V_{ket}, and pyruvate (and lactate) blood–brain exchange, V_{ex}, both of which contribute unlabeled carbons to the acetyl-CoA pool. V_{out} represents a net efflux of pyruvate (and lactate) into the blood. Under these conditions, the mass balance between V_{TCA} and $CMR_{glc}(total)$, based on the fact that a hexose forms two trioses, is given by

$$CMR_{glc}(total) = \tfrac{1}{2} \times [V_{TCA} - V_{ket} + V_{out}], \quad [3]$$

where the oxidative and nonoxidative portions are

$$CMR_{glc}(oxidative) = \tfrac{1}{2} \times [V_{TCA} - V_{ket}], \quad [4]$$

$$CMR_{glc}(nonoxidative) = \tfrac{1}{2} \times V_{out}. \quad [5]$$

Although V_{out} was not measured in the study, comparison of $CMR_{glc}(oxidative)$ from this study with $CMR_{glc}(total)$ from the autoradiography study (4), both at rest and during stimulation, will allow the determination of V_{out} [i.e., $CMR_{glc}(nonoxidative)$ as in Eq. **5**]. Likewise, the stoichiometry between V_{TCA} and CMR_{O2} is given by

$$CMR_{O2} = 3 \times [2 \times CMR_{glc}(total) - V_{out}] + 2.25 \times V_{ket}, \quad [6]$$

where the different factors for $[2 \times CMR_{glc}(total) - V_{out}]$ and V_{ket} in Eq. **6** signify that different precursors for acetyl-CoA (i.e., glucose and ketone bodies) are coupled differently to oxidative metabolism (12, 13). Substituting Eq. **3** into Eq. **6** results in

$$CMR_{O2} = 3 \times V_{TCA} - 0.75 \times V_{ket}, \quad [7]$$

which calculates the oxygen consumption from the TCA cycle. Therefore, for each value of V_{TCA} the values of $CMR_{glc}(oxidative)$ and CMR_{O2} were calculated from Eqs. **4** and **7**, respectively. Dilution of the acetyl-CoA pool, V_{dil}, is given by

$$V_{dil} = V_{TCA} \times [1 - (\text{C4-glutamate}^{13}\text{CFE}/\tfrac{1}{2}\cdot\text{C1-glucose}\ ^{13}\text{C FE})], \quad [8]$$

provided that enrichment of the glutamate pool has reached steady state, as observed in this study. Parameters determined from the data, including the fit to the model, are V_{TCA} and C4-glutamate ^{13}C FE/½·C1-glucose ^{13}C FE. The modelling was performed with either (*i*) $V_{ket} = V_{dil}$ and $V_{ex} = 0$ or (*ii*) $V_{ex} = V_{dil}$ and $V_{ket} = 0$. All data are presented as mean ± SD.

RESULTS

Activation of the Motor and Somatosensory Areas. During double forepaw stimulation, the fMRI data showed that the activated volume of tissue was bilateral and in the range of 45–60 mm^3 (data not shown), encompassing the motor and somatosensory areas (Fig. 2). The image-contrast in the fMRI experiment is BOLD (25). Therefore, the volume of interest for the POCE NMR measurement was chosen as a 50-mm^3 rectangular box centered in the motor, somatosensory, or occipital areas of the cortex. The occipital area was chosen as a control region of nonactivated tissue for the POCE study because fMRI showed no activation in this region (11). The BOLD signal-change ($\Delta S/S$) remained elevated throughout the 1-h stimulation (see Fig. 2). For a particular coronal slice, the area of the activated region measured at 20-min intervals showed <20% variation during the 1-h stimulation period (data not shown). Possible artifacts from blood vessels and head movements were found to be negligible (11).

Changes in V_{TCA} During Forepaw Stimulation. The plasma glucose concentration was increased during infusion from a basal value of ≈7 mM to ≈15 mM. An approximate 50% ^{13}C FE of plasma C1-glucose was obtained within 5 min from the start of infusion (Table 1) and maintained throughout the infusion period. Effects of increased plasma glucose on the concentrations of brain metabolites were assessed by subtraction of ^{1}H NMR spectra obtained before and during glucose infusion. No changes were observed in the brain content of glutamate, glutamine, *N*-acetylaspartate, choline, and total creatine (data not shown).

Serial spectra of C4-glutamate (2.35 ppm) obtained from the somatosensory region of the brain of a resting and stimulated rat are shown in Fig. 3. The C4-glutamate signal increased more rapidly in stimulated rats (Fig. 3*B*) than in resting rats (Fig. 3*A*). The POCE data presented here represent a 4-fold enhancement in sensitivity over our previous study (9), as a consequence of localized shimming, better radio-frequency surface-coil design, and lower noise preamplifiers. Subtraction errors from scalp lipids occasionally observed in the 1- to 1.5-ppm region did not interfere with the C4-glutamate measurement.

The time courses of C4-glutamate labeling and the fits of the metabolic model to the data for four rats are shown in Fig. 4. During stimulation, there was a significant increase in the rate of C4-glutamate labeling in the somatosensory area (Fig. 4 *A* and *B*). The mean values of V_{TCA} measured in the somatosensory area increased from 0.49 ± 0.03 to 1.48 ± 0.82 μmol/g/min ($P < 0.01$) during stimulation (see Table 1). An increase in the mean value of V_{TCA} was also measured in the motor area (resting, 0.35 ± 0.06; stimulation, 0.54 ± 0.10 μmol/g/min; $P < 0.03$; see Table 1). The percentage increases in V_{TCA} within the somatosensory and motor areas were 202% and 54%, respectively (see Table 1). In contrast, during stimulation, there was no significant increase in the rate of C4-glutamate labeling in the occipital area (Fig. 4 *C* and *D*). The mean values of V_{TCA} did not change significantly in the

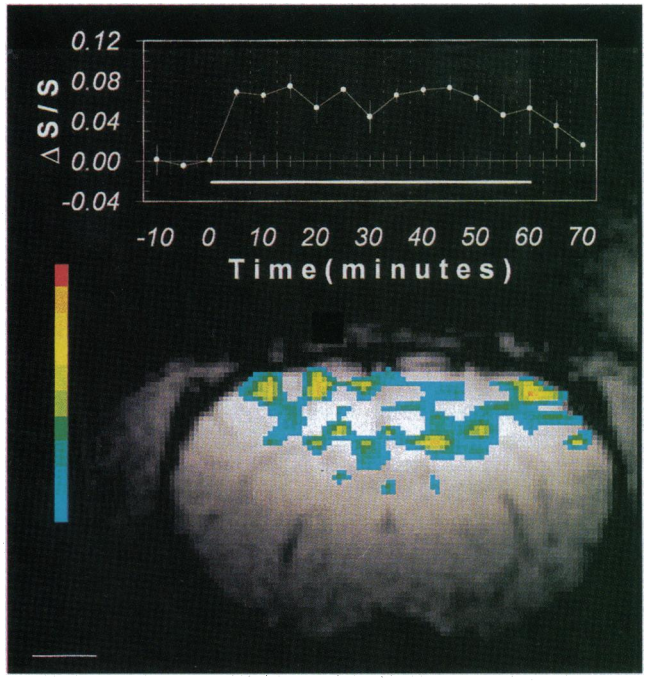

FIG. 2. Bilateral activation of somatosensory and motor areas (represented by a *t*-map[11]) during double forepaw stimulation shown in a coronal slice ≈1 mm anterior to the bregma. The multislice echo-planar imaging fMRI data showed that the activated volume of tissue, determined as described (11), was 45–60 mm^3. The increased blood-oxygenation level dependent (BOLD; ref. 25) signal change ($\Delta S/S$) remained elevated throughout the duration of the stimulation period (1 h), and the average $\Delta S/S$ in the right (shown) and left regions of interest [defined as a 1-mm^2 region ± 2.5 mm from the midline] were 0.07 ± 0.01 and 0.09 ± 0.02 ($n = 4$), respectively. The *t*-map is thresholded with $P < 0.005$ (blue/green), and the increments in the color bar are $t_{.995}$, $t_{.996}$, $t_{.997}$, $t_{.998}$, etc. (Bar = 2 mm.)

occipital area during stimulation (resting, 0.42 ± 0.11; stimulation, 0.36 ± 0.17 μmol/g/min; $P > 0.30$; see Table 1). A greater variability in V_{TCA} was observed during stimulation compared with the resting condition in the motor and somatosensory areas, resulting in larger errors shown in Table 1. Some of this variation may be due to the faster labeling of glutamate, which results in fewer data points during the most rapidly changing part of the labeling time course (see Fig. 4*B*). The variability could also be due to differences in positioning of the volume of interest and/or variations in placement of electrodes in the forepaw, which could have caused differences in the localization and/or sizes of activated tissue volume (Fig. 2).

For the results shown in Fig. 4 and summarized in Table 1, modelling was carried out with $V_{max}/CMR_{glc} = 5.8$ and a V_{gln} value of 0.08 μmol/g/min. To investigate the dependence of V_{TCA} on the rate of glucose transport, each modelling was also carried out with $V_{max}/CMR_{glc} = 23.2$, and the results obtained for V_{TCA} were 10–15% less than the results shown in Table 1. These values represent the range of V_{TCA} expected from either slow or rapid glucose transport (16). To investigate the dependence of V_{TCA} on the rate of glutamate–glutamine exchange, modelling was also carried out with $V_{gln} = 0.44$ μmol/g/min, and the results obtained for V_{TCA} were 10–20% greater than the results shown in Table 1. These values represent the range of V_{TCA} expected from either slow or rapid exchange between the glutamate and glutamine (12, 13).

For the resting animals, a time lag of 4–10 min was observed before the appearance of significant C4-glutamate labeling (see Fig. 3*A*), and this time lag is consistent with brain glucose levels of 2–4 μmol/g under the assumption that brain glucose kinetics are the same as that previously measured under nitrous oxide (16). The absence of the time lag in the stimulated rats (see Fig. 3*B*) is consistent with a higher value of $CMR_{glc}(oxidative)$ during forepaw stimulation, which in turn would reduce the brain glucose concentration (18), resulting in a faster ^{13}C isotopic turnover of the brain glucose pool.

Dilution of the Acetyl-CoA Pool. In this study, since it was found that the ^{13}C FE of C4-glutamate is less than half that of C1-glucose (see Table 1), the extent of total dilution of the acetyl-CoA pool was determined by Eq. **8** (9, 24). An approximate mean value of $0.25 \times V_{TCA}$ was estimated for V_{dil} in this study (see Table 1). Since the rats in this study were fasted for ≈24 h, the dilution source may have large contributions from ketone bodies. However, the pyruvate (and lactate) blood–brain exchange may have made significant contributions of unlabeled carbons to the TCA cycle via the acetyl-CoA pool. Therefore, two scenarios of dilution of the acetyl-CoA pool were examined by metabolic modelling for the determination of $CMR_{glc}(oxidative)$ and CMR_{O2}, using Eqs. **4** and **7**, respectively: (*i*) the total dilution source is from the ketone bodies (i.e., $V_{ket} = V_{dil} = 0.25 \times V_{TCA}$ and $V_{ex} = 0$) and (*ii*) the total dilution is due to pyruvate (and lactate) blood–brain exchange (i.e., $V_{ex} = V_{dil} = 0.25 \times V_{TCA}$ and $V_{ket} = 0$).

For 24-h fasted rats, as used in this study, ≈12% of unlabeled carbon flow into the TCA cycle is from ketone bodies (24) while an additional 10–15% dilution can be accounted for from pyruvate (and lactate) exchange (26, 27). Small but negligible dilutions may be caused by the pentose phosphate shunt (≈1% calculated from ref. 28) and degradation of proteins (<1% calculated from ref. 29). Therefore, the total dilution expected from all sources is ≈25% for 24-h fasted rats, which is in excellent agreement with the total dilution of the acetyl-CoA pool determined in this study (i.e., $V_{dil} = 0.25 \times V_{TCA}$).

Changes in $CMR_{glc}(oxidative)$ and CMR_{O2}. For each value of V_{TCA}, a value for $CMR_{glc}(oxidative)$ was calculated based on Eq. **4**. When $V_{ket} = V_{dil}$ and $V_{ex} = 0$, in the somatosensory area, the mean value of $CMR_{glc}(oxidative)$ increased from 0.19 ± 0.02 to 0.56 ± 0.31 μmol/g/min ($P < 0.01$) during stimulation (see Table 1). In the motor area, an increase in $CMR_{glc}(oxidative)$ was also measured [0.14 ± 0.02 (rest) and 0.20 ± 0.04 (stimulation) μmol/g/min; $P < 0.03$; see Table 1]. In the somatosensory and motor areas, the percentage increases in $CMR_{glc}(oxidative)$ were 195% and 43%, respectively, similar to the magnitude of changes for V_{TCA} (202% and 54%, respectively; see Table 1). In the occipital area, the mean value of $CMR_{glc}(oxidative)$ did not change significantly upon stimulation [0.16 ± 0.04 (rest) and 0.14 ± 0.07 (stimulation) μmol/g/min; $P > 0.30$; see Table 1]. Almost identical trends were observed for $CMR_{glc}(oxidative)$ values when $V_{ex} = V_{dil}$ and $V_{ket} = 0$, as shown in Table 1.

Table 1. Summary of results (motor, somatosensory, and occipital areas in resting and stimulated rats)

	glc ^{13}C FE	glu ^{13}C Fe	Dilution[a]	V_{TCA}	CMR_{O2}[b]	CMR_{02}[c]	CMR_{glc}[d]	CMR_{glc}[e]	lit. CMR_{glc}[f]
Motor									
Resting ($n = 2$)	49.6 ± 1.9%	17.1 ± 1.3%	0.31 ± 0.04	0.35 ± 0.06	0.98 ± 0.16	1.05 ± 0.17	0.14 ± 0.02	0.18 ± 0.3	—
Stimulation ($n = 2$)	52.9 ± 5.7%	19.2 ± 2.4%	0.27 ± 0.04	0.54 ± 0.10[g]	1.52 ± 0.23[g]	1.62 ± 0.24[g]	0.20 ± 0.03[g]	0.27 ± 0.05[g]	—
Somatosensory									
Resting ($n = 4$)	56.6 ± 4.4%	20.0 ± 1.4%	0.29 ± 0.03	0.49 ± 0.03	1.38 ± 0.17	1.47 ± 0.18	0.19 ± 0.02	0.25 ± 0.03	0.25 ± 0.05[i]
Stimulation ($n = 7$)	47.3 ± 6.0%	18.4 ± 2.3%	0.22 ± 0.05	1.48 ± 0.82[h]	4.16 ± 2.29[h]	4.44 ± 2.44[h]	0.56 ± 0.31[h]	0.74 ± 0.41[h]	0.53–0.95[j]
Occipital									
Resting ($n = 3$)	53.8 ± 6.8%	19.6 ± 2.2%	0.27 ± 0.05	0.42 ± 0.11	1.18 ± 0.32	1.26 ± 0.34	0.16 ± 0.04	0.21 ± 0.06	0.17 ± 0.06[l]
Stimulation ($n = 3$)	50.4 ± 6.6%	17.9 ± 2.1%	0.29 ± 0.05	0.36 ± 0.17[k]	1.01 ± 0.54[k]	1.08 ± 0.58[k]	0.14 ± 0.07[k]	0.18 ± 0.09[k]	—

Flux values are in units of μmol/g/min. glc, C1-glucose; glu, C4-glutamate; dilution, dilution of the acetyl-CoA pool.

[a]dilution of the acetyl-CoA pool was calculated by [1 − (C4-glutamate ^{13}C FE/½·C1-glucose ^{13}C (FE)].

[b]CMR_{O2} calculated by Eq. **7** with $V_{ket} = V_{dil} = 0.25 \times V_{TCA}$ and $V_{ex} = 0$ (dilution from ketone bodies).

[c]CMR_{O2} calculated by Eq. **7** with $V_{ex} = V_{dil} = 0.25 \times V_{TCA}$ and $V_{ket} = 0$ [dilution from pyruvate (and lactate) exchange].

[d]$CMR_{glc} = CMR_{glc}(oxidative)$ calculated by Eq. **4** with $V_{ket} = V_{dil} = 0.25 \times V_{TCA}$ and $V_{ex} = 0$ (dilution from ketone bodies).

[e]$CMR_{glc} = CMR_{glc}(oxidative)$ calculated by Eq. **4** with $V_{ex} = V_{dil} = 0.25 \times V_{TCA}$ and $V_{ket} = 0$ [dilution from pyruvate (and lactate) exchange].

[f]lit. $CMR_{glc} = CMR_{glc}(total)$ measured by autoradiography, which is equal to $CMR_{glc}(oxidative) + CMR_{glc}(nonoxidative)$, as shown in Eq. **3**.

[g]$P < 0.03$ (in comparison to resting data for motor area).

[h]$P < 0.01$ (in comparison to resting data for somatosensory area).

[i]Data from ref. 4.

[j]Data from ref. 4. The actual value reported by Ueki and coworkers (4) was 0.39 ± 0.10 μmol/g/min for the entire somatosensory area. Our previous fMRI results of single forepaw stimulation (11) and a rat limb placement study (27) showed that ≤½ of the anterior part of the somatosensory area is activated during forepaw stimulation. Therefore, when allowances are made for partial volume averaging of activated tissue within the entire somatosensory area (20–50%), the value of CMR_{glc} (total) during stimulation as reported by Ueki and coworkers (4) would rise to 0.53–0.95 μmol/g/min. The same reasoning applies for the reported CBF values (1.20–1.91 ml/g/min during stimulation and 0.72 ml/g/min at rest).

[k]$P > 0.30$ (in comparison to resting data for occipital area).

[l]Data from ref. 31.

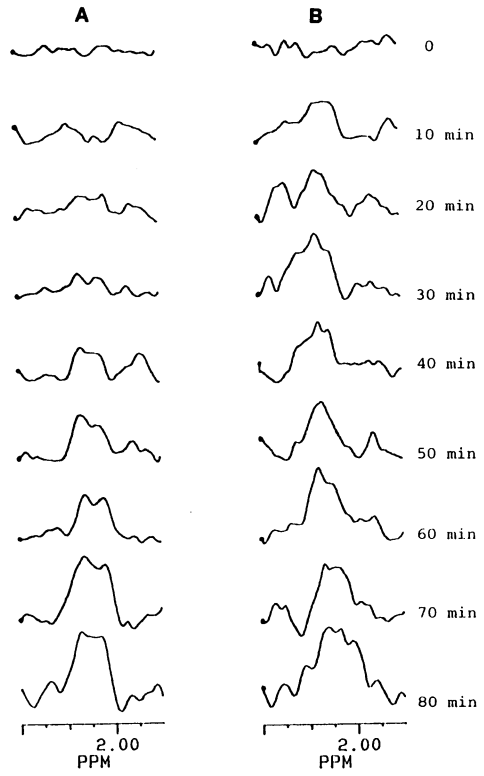

FIG. 3. Typical POCE difference spectra, from the somatosensory area, showing the time courses of C4-glutamate signal for resting (*A*) and stimulated (*B*) rats. Each increment in the horizontal axis of a spectrum is 0.25 ppm. The chemical shift of C4-glutamate is 2.35 ppm. These spectra were exponentially line-broadened by 20 Hz. A comparison of *A* and *B* shows that the C4-glutamate signal reaches steady levels much more rapidly in the stimulated rats, thus indicating a faster TCA cycle flux in the somatosensory area during forepaw stimulation (see Fig. 4 and Table 1). The peak at 2.11 ppm is C3-glutamate.

For each value of V_{TCA}, a value for CMR_{O2} was calculated based on Eq. **7**. The results are summarized in Table 1. When $V_{ket} = V_{dil}$ and $V_{ex} = 0$, in the somatosensory and motor areas, the percentage increases in CMR_{O2} were 201% and 55% (see Table 1). In contrast, in the occipital area, CMR_{O2} did not change significantly during stimulation [1.18 ± 0.32 (rest) and 1.01 ± 0.54 (stimulation) μmol/g/min; $P > 0.30$; see Table 1]. Similar trends were observed for CMR_{O2} values when $V_{ex} = V_{dil}$ and $V_{ket} = 0$ (see Table 1).

DISCUSSION

Ueki and coworkers (4) showed that, upon electrical stimulation of the rat forepaw under α-chloralose anesthesia, there is an increase in CBF and CMR_{glc} in the contralateral somatosensory area. Recently, we reported similar localized activation with fMRI during single forepaw stimulation (11), and in the present study, the fMRI results showed bilateral activation of the motor and somatosensory areas during double forepaw stimulation (see Fig. 2). Furthermore, we have obtained values for V_{TCA}, CMR_{glc}(*oxidative*), and CMR_{O2} for the resting and stimulated rat (see *Results*) to test the hypothesis that the additional energy required for brain activation is provided through nonoxidative glycolysis (2, 3).

In this study, the minimum fraction of C4-glutamate derived from C1-glucose was ≈75% (see Table 1). The effect of unlabeled carbon precursors, such as β-hydroxybutyrate, will result in a small adjustment of the stoichiometry between V_{TCA} and CMR_{O2} or CMR_{glc}(*oxidative*) (see Eqs. **4** and **7**; Table 1). For the resting rat, the mean value of CMR_{glc}(*oxidative*) in the somatosensory area determined in this study (0.19 ± 0.02 μmol/g/min) is in good agreement with the reported value of CMR_{glc}(*total*) by Ueki and coworkers (4) (0.25 ± 0.05 μmol/g/min), as shown in Table 1. For the stimulated rat, to compare the CMR_{glc}(*oxidative*) value from this study to the reported value by Ueki and coworkers (4), it was necessary to correct their reported value of CMR_{glc}(*total*), which reflected metabolism for the entire somatosensory cortex and not for the fraction of the cortex that was activated (see Table 1). The ratio of the activated volume to the total volume of the somatosensory area was estimated from our fMRI results (in ref. 11 and this study) to be 20–50%. When this correction is made, the comparison of CMR_{glc}(*oxidative*) from this study (0.56 ± 0.31 μmol/g/min) is in good agreement with the value of CMR_{glc}(*total*) by Ueki and coworkers (ref. 4; 0.53–0.95 μmol/g/min), as shown in Table 1. For the somatosensory area, the increase in CMR_{O2} observed in the present study (201%) is comparable to the increases in CMR_{glc}(*oxidative*) from this study (195%) and CMR_{glc}(*total*) from Ueki and coworkers (ref. 4; 112–280%), as shown in Table 1.

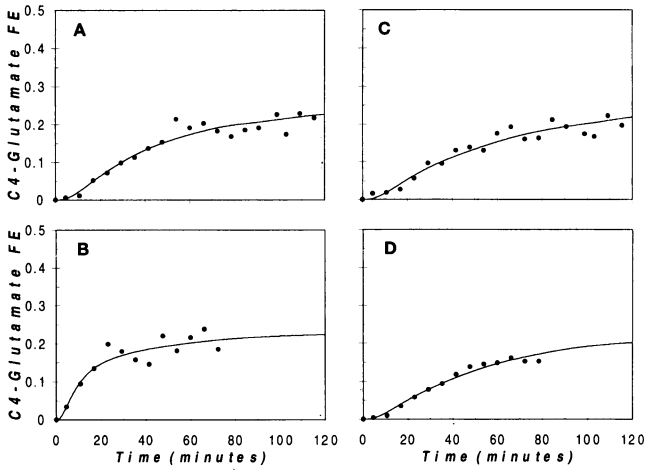

FIG. 4. From four separate studies, the C4-glutamate time courses obtained from POCE data (●) and the best fits of the metabolic model to the data (line). The vertical axis is the C4-glutamate ^{13}C FE in the brain and the horizontal axis is the time of C1-glucose infusion. For the stimulated animals, the stimulation was begun before the start of infusion. In the somatosensory area, the value of V_{TCA} was 0.49 ± 0.08 μmol/g/min at rest (*A*) and 1.28 ± 0.34 μmol/g/min during forepaw stimulation (*B*). In the occipital area, the value of V_{TCA} was 0.48 ± 0.08 μmol/g/min at rest (*C*) and 0.53 ± 0.07 μmol/g/min during forepaw stimulation (*D*). See Table 1 for details.

Whether the dilution of the acetyl-CoA pool is from ketone bodies and/or pyruvate (and lactate) exchange, values of CMR_{glc}(*oxidative*) obtained in the present study are in good agreement with reported values of CMR_{glc}(*total*), at rest and during stimulation (see Table 1). More importantly, the agreement between the values of CMR_{glc}(*oxidative*) obtained during forepaw stimulation in this study and the value of CMR_{glc}(*total*) by Ueki and coworkers (4) shows that any additional glucose consumption by nonoxidative glycolysis is small so that any contribution to the total energy supplied is insignificant (1, 7). Since within the error of comparisons, we can rule out net loss of pyruvate (and lactate) into the blood from the brain (i.e., $V_{out} \approx 0$ in Fig. 1; see Eq. **5**), this study shows that the majority of the energy for brain activation during sustained rat forepaw stimulation is supplied by oxidative glycolysis.

The initial rate of C4-glutamate labeling depends on the size of metabolite intermediate pools between plasma glucose and glutamate of which brain glucose and lactate are the largest (see refs. 12 and 13). The effect of these intervening pools is to delay the ^{13}C FE time course of C4-glutamate relative to enrichment time course of plasma C1-glucose, as shown by the significant time lag for a resting rat (see Fig. 4*A*). The major

pool contributing to this time lag is intracellular glucose, which was calculated from glucose transport parameters measured in a previous ^{13}C NMR study (16). Since the previous study was carried out under nitrous-oxide anesthesia, we examined the impact of the glucose transport kinetics on the results. For the results shown in Fig. 4 and Table 1, the modelling was carried out with maximum glucose transport (V_{max}) of 1.16 μmol/g/min (i.e., V_{max}/CMR_{glc} = 5.8), which is based on parameters determined under nitrous oxide anesthesia. The assumption of this modelling was that glucose transport and metabolism were down-regulated by the same fraction under α-chloralose anesthesia, as used in this study. When the modelling was carried out under the other extreme of no transport down-regulation with V_{max}= 4.64 μmol/g/min (i.e., V_{max}/CMR_{glc} = 23.2), the results obtained for V_{TCA}, $CMR_{glc}(oxidative)$, and CMR_{O2} were 10–15% less than the results shown in Table 1. The percentage changes in fluxes were similar in these two extreme cases of glucose transport parameters.

The large increase in CMR_{O2} during forepaw stimulation raises the question of whether oxygen delivery may limit the energy available for brain activation. The value of CMR_{O2} determined in this study may be combined with previous measurements of CBF (as in ref. 4) to estimate the glucose and oxygen extraction fractions (i.e., E_{glc} and E_{O2}). In the resting condition, CBF in the nonactivated somatosensory cortex under similar conditions of anesthesia has been reported (4) to be 0.72 ml/g/min with an arterial oxygen content of 7.5 μmol/ml. As a consequence of the plasma glucose infusion in the present study, the arterial glucose concentration was 14.5 μmol/ml. These values indicate that glucose and oxygen availability (i.e., A_{glc} and A_{O2}), where availability is defined as the product of CBF and arterial concentration of glucose or oxygen (1), were 10.5 and 5.4 μmol/g/min, respectively. In the somatosensory area, the values of $CMR_{glc}(oxidative)$ and CMR_{O2} for the resting rat determined in this study were 0.19 and 1.38 μmol/g/min (see Table 1), respectively. Thus, the glucose and oxygen extraction fractions E_{glc} and E_{O2}, which are defined (1) as $CMR_{glc}(oxidative)/A_{glc}$ and CMR_{O2}/A_{O2}, are 2% and 26%, respectively, at rest. Upon forepaw stimulation, the values of $CMR_{glc}(oxidative)$ and CMR_{O2} in the somatosensory area were 0.56 and 4.16 μmol/g/min (see Table 1), respectively, and the CBF was in the range of 1.20–1.91 ml/g/min (see Table 1). The corresponding values of E_{glc} and E_{O2} are 2–3% and 29–46%, respectively, upon stimulation. These extraction rates during the resting and stimulated conditions are within the capacity of the brain to extract the respective nutrients from the blood (1). It is extremely unlikely that the glucose supply becomes limiting during sustained brain activation. However, it is possible that the oxygen supply could become limiting in some situations (1, 32). The observation of a positive BOLD signal change in the fMRI experiments throughout the 1-h long stimulation period (see Fig. 2), despite a 200% change in oxidative metabolism during forepaw stimulation, indicates that the local change in CBF needs to be slightly greater than the change in CMR_{O2} (see ref. 26). Given the changes in CBF from Ueki and coworkers (4) and CMR_{O2} from this study, it is not inconsistent with a positive BOLD signal-change. However, future experiments with simultaneous measurements of CBF and CMR_{O2} on the same rat are needed to clarify this issue.

A small increase in lactate concentration occurs during rat forepaw stimulation (4) suggesting that nonoxidative glycolysis contributes to the energy required for brain activation. However, given the much greater efficiency of ATP production from glucose oxidation compared with glycolysis (1, 7), the small increase in lactate observed by Ueki and coworkers (4) under these conditions would not provide a substantial fraction of the energy required for brain activation. Functional ^1H NMR spectroscopy of the lactate time course from the human occipital cortex (5, 6) indicates that the lactate is produced within the first few minutes of activation (5, 6, 33). During this transient period, a larger fraction of the energy required for cortical activation may be provided by nonoxidative glycolysis and possibly by use of high-energy phosphate compounds such as phosphocreatine. However, the present results suggest that, under conditions of sustained cortical sensory activation in rat brain, the energy required is provided mainly by the oxidation of glucose.

F.H. and R.G.S. would like to thank Prof. K. A. Hossmann (Max Planck Institute of Neurological Research, Köln, Germany) for a careful reading of the manuscript. We thank T. Nixon and P. Brown for technical support. This work was supported by National Institutes of Health Grants DK-27121, RR-07723 (G.F.M.), and HD-32573 (K.L.B.), and by FIRST Award NS-32126 (D.L.R.). F.H. acknowledges the Society of Cerebral Blood Flow and Metabolism for the Young Scientist's Award (1995).

1. Siesjö, B. K. (1978) *Brain Energy Metabolism* (Wiley, New York).
2. Fox, P. T. & Raichle, M. E. (1986) *Proc. Natl. Acad. Sci. USA* **83,** 1140–1144.
3. Fox, P. T., Raichle, M. E., Mintun M. A. & Dence, C. (1988) *Science* **241,** 462–464.
4. Ueki, M., Linn, F. & Hossman, K. A. (1988) *J. Cereb. Blood Flow Metab.* **8,** 486–494.
5. Prichard, J. W., Rothman, D. L., Novotny, E. J., Petroff, O. A. C., Kuwabara, T., Avison, M. J., Howseman, A. M., Hanstock, C. C. & Shulman, R. G. (1991) *Proc. Natl. Acad. Sci. USA* **88,** 5829–5831.
6. Sappey-Marinier, D., Calabrese, G., Fein, G., Hugg, J. W., Biggins, C. & Weiner M. W. (1992) *J. Cereb. Blood Flow Metab.* **12,** 584–592.
7. Shulman, R. G., Blamire, A. M., Rothman, D. L. & McCarthy, G. (1993) *Proc. Natl. Acad. Sci. USA* **90,** 3127–3133.
8. Rothman, D. L., Behar, K. L., Hetherington, H. P., den Hollander, J. A., Bendall, M. R., Petroff, O. A. C. & Shulman, R. G. (1985) *Proc. Natl. Acad. Sci. USA* **82,** 1633–1637.
9. Fitzpatrick, S. M., Hetherington, H. P., Behar, K. L. & Shulman, R. G. (1990) *J. Cereb. Blood Flow Metab.* **10,** 170–179.
10. Rothman, D. L., Novotny, E. J., Shulman, G. I., Howseman, A. M., Petroff, O. A. C., Mason, G. F., Nixon, T. W., Hanstock, C. C., Prichard, J. W. & Shulman, R. G. (1992) *Proc. Natl. Acad. Sci. USA* **89,** 9603–9606.
11. Hyder, F., Behar, K. L., Martin, M. A., Blamire, A. M. & Shulman, R. G. (1994) *J. Cereb. Blood Flow Metab.* **14,** 649–655.
12. Mason, G. F., Rothman, D. L., Behar, K. L. & Shulman, R. G. (1992) *J. Cereb. Blood Flow Metab.* **12,** 434–447.
13. Mason, G. F., Gruetter, R., Rothman, D. L., Behar, K. L., Shulman, R. G. & Novotny, E. J. (1995) *J. Cereb. Blood Flow Metab.* **15,** 12–25.
14. Hyder, F, Chase, J. R., Behar, K. L., Mason, G. F., Rothman, D. L. & Shulman, R. G. (1995) *J. Cereb. Blood Flow Metab.* **15,** S76.
15. Behar, K. L., Petroff, O. A. C., Prichard, J. W., Alger, J. R. & Shulman, R. G. (1986) *J. Magn. Reson. Med.* **3,** 911–920.
16. Mason, G. F., Behar, K. L., Rothman, D. L. & Shulman, R. G. (1992) *J. Cereb. Blood Flow Metab.* **12,** 448–455.
17. Hyder, F., Rothman, D. L. & Blamire, A. M. (1995) *Magn. Reson. Imaging* **13,** 97–103.
18. Chen, W., Novotny, E. J., Zhu, X.-H., Rothman, D. L. & Shulman, R. G. (1993) *Proc. Natl. Acad. Sci. USA* **90,** 9896–9900.
19. Gruetter, R. (1993) *Magn. Reson. Med.* **29,** 804–811.
20. Ordidge, R. J., Connelly, A. & Lohman, A. B. (1986) *J. Magn. Reson.* **66,** 283–294.
21. Zilles, K. (1985) *The Cortex of the Rat: A Stereotaxic Atlas* (Springer, New York).
22. Martin, M. A., Mason, G. F., Behar, K. L. & Shulman, R. G. (1995) *Soc. Magn. Reson. Abstr.* **3,** 1783.
23. Hawkins, R. A. & Mans, A. M. (1983) *Handbook of Neurochemistry,* ed. Lajtha, A. (Plenum, New York), Vol. 3, pp. 259–294.
24. Mason, G. F., Martin, M. A., Behar, K. L. & Shulman, R. G. (1993) *Soc. Magn. Reson. Abstr.* **3,** 1513.
25. Ogawa, S., Menon, R. S., Tank, D. W., Kim, S. G., Merkle, H., Ellermann, J. M. & Ugurbil, K. (1993) *Biophys. J.* **64,** 803–812.
26. Pardridge, W. M. & Oldendorf, W. H. (1977) *J. Neurochem.* **28,** 5–12.
27. Hawkins, R. A., Mans, A. M., Davis, D. W., Vina, J. R. & Hibbard, L. S. (1985) *Am. J. Physiol.* **248,** C170–C176.
28. Gaitonde, M. K., Evison, E. & Evans, G. M. (1983) *J. Neurochem.* **41,** 1252–1260.
29. Berl, S., Lajtha, A. & Waelsch., H. (1961) *J. Neurochem.* **7,** 186–197.
30. De Ryck, M., Van Reempts, J., Duytschaever, H., Van Deuren, B. & Clincke, G. (1992) *Brain Res.* **573,** 44–60.
31. Dudley, R. E., Nelson, S. E. & Samson, F. (1982) *Brain Res.* **233,** 173–180.
32. Lenigert-Follert, E. (1984) *Advances in Experimental Medicine and Biology* (Plenum, New York), Vol. 191, pp. 3–19.
33. Frahm, J., Kruger, G., Merboldt, K. D. & Kleinschmidt, A. (1996) *Magn. Reson. Med.* **35,** 143–148.